Application of Multi-Objective PSO Algorithm for Power System Stability Enhancement by Means of PSS and SVC

Yosra WELHAZI[1], Tawfik GUESMI[2], Hsan HADJ ABDALLAH[3]

National Engineering School of Sfax, Sfax University, B.P.W.3038 Sfax, Tunisia

[1]yosrawelhazi@yahoo.fr
[2]tawfik.guesmi@istmt.rnu.tn
[3]hsan.haj@enis.rnu.tn

Abstract— **In this paper, we present method for enhancement of power system stability via robust coordinated design of a power system stabilizer (PSS) and a static VAR compensator (SVC)-based stabilizer. The coordinated design problem of PSS and SVC-based controllers can be formulated as an optimization problem with integral of time-multiplied absolute value of the error square (ITAE)-based objective function. The multi-objective particle swarm optimization (MOPSO) is employed to search for optimal controller parameters. To ensure the robustness of the proposed controllers, the design process takes into account a wide range of operating conditions. This study also presents singular value decomposition (SVD)-based approach to evaluate the potential of controllers to enhance the dynamic stability of power system. The proposed stabilizers are tested on a single machine infinite bus (SMIB). The effectiveness and robustness of the proposed approach is demonstrated through the nonlinear simulation results, eigenvalue analysis and controllability measure over a wide range of loading conditions.**

Keywords— **Power system stabilizer, Static VAR compensator, Multi-objective particle swarm optimization, Singular value decomposition, Single machine infinite bus.**

I. INTRODUCTION

When large power systems are interconnected by relatively weak tie lines, low frequency oscillations have been observed. These oscillations may sustain and grow to cause system separation if no adequate damping is available [1]. In order to damp these power system oscillations and increase system oscillations stability, the conventional power system stabilizer (CPSS) is widely used by power system utilities. In general, the function of the CPSS is to produce component of electrical torque in phase with the rotor speed deviations. However, PSSs suffer a drawback of being liable to cause great variations in the voltage profile and they may even result in leading power factor operation under severe disturbances. In recent years, the advances in power electronics have contributed to the development of flexible alternating current transmission systems (FACTS) [2]. FACTS devices are used to improve power system stability in addition to their primary application in the power flow control. Recently, several works have been done on the coordination of power system stabilizer (PSS) and FACTS-based stabilizers in order to enhance power system stability [3-5]. This problem of coordination consists to tune the FACTS and PSS parameters. Static VAR compensator (SVC) is one of the important members of FACTS family which can be installed in parallel in the transmission lines. In the literature [6,7], the coordinated design of PSS and SVC is formulated as a nonlinear multiobjective problem. A number of conventional techniques have been reported in the literature to solve this design problem such as mathematical programming and gradient procedure for optimization. Unfortunately, the conventional techniques are time consuming as they are iterative and require heavy computation burden and slow convergence. In addition, the search process is susceptible to be trapped in local minima and the solution obtained may not be optimal [8]. To overcome these problems, heuristic algorithms are employed for solving optimization problems such as particle swarm optimization (PSO) [9] and tabu search algorithm (TS) [10]. The advantage of these methods is their ability to avoid entrapment in local optimal solution and prevent cycling by using flexible memory of search history.

In this paper, the multi-objective particle swarm optimization (MOPSO) [11] is employed to search for the optimal settings of stabilizer parameters and generate the Pareto optimal solutions. A controllability measure-based singular value decomposition (SVD) is used to select the control signal which is most suitable for damping the electromechanical mode oscillations. The effectiveness and robustness of the proposed stabilizers to enhance system dynamic stability is demonstrated through controllability measure, eigenvalue analysis and nonlinear time-domain simulation studies. Results evaluation show that the proposed multi-objective function achieves good robust performance for a wide range of operating conditions.

II. POWER SYSTEM MODEL

A. Generator Model

A single machine infinite bus (SMIB) system is considered in this study as shown in Fig.1. The generator is equipped with PSS and the system has an SVC at the midpoint of the line. The line equivalent impedance is $Z = R + jX$ and the

ISSN: 2356-5608

generator has a local load of admittance $Y = G + jB$. The generator is described by third-order model: two equations of motion and the generator internal voltage equation.

$$\dot{\delta} = \omega_b(\omega - 1) \tag{1}$$

$$\dot{\omega} = (P_m - P_e - D(\omega - 1))/M \tag{2}$$

$$\dot{E}'_q = (E_{fd} - (x_d - x'_d)i_d - E'_q)/T'_{d0} \tag{3}$$

Where ω and δ are the rotor speed and angle, respectively; P_e and P_m are the electrical and mechanical powers of the generator, respectively; D and M are the damping coefficient and inertia constant, respectively; E_{fd} and E'_q are the field and internal voltages, respectively; T'_{d0} is the open circuit field time constant; x'_d and x_d are d-axis transient reactance and d-axis reactance of the generator, respectively.

The output generator power can be presented as follows:

$$P_e = v_d i_d + v_q i_q \tag{4}$$

Where:

$$v_d = x_q i_q \tag{5}$$

$$v_q = E'_q - x'_d i_d \tag{6}$$

Here, v_d and v_q are the d-axis and q-axis components of the terminal voltage, respectively; i_d and i_q are the d-axis and q-axis components of the armature current, respectively; x_q is the q-axis reactance of the generator.

Using Eqs. (4) −(6) the electrical power can be written as:

$$P_e = E'_q i_q + (x_q - x'_d) i_d i_q \tag{7}$$

The generator terminal voltage is:

$$v_t^2 = v_d^2 + v_q^2 \tag{8}$$

B. Exciter and PSS Controller

The IEEE Type-ST1 excitation system shown in Fig.2 is considered in this study. It can be described as:

$$\dot{E}_{fd} = (K_A(V_{ref} - v_t + u_{PSS}) - E_{fd})/T_A \tag{9}$$

Where K_A and T_A are the gain and time constant of the excitation system, respectively; V_{ref} is the reference voltage.

As shown in Fig.2, a conventional lead-lag PSS is installed in the feedback loop to generate a stabilizing signal u_{PSS} .

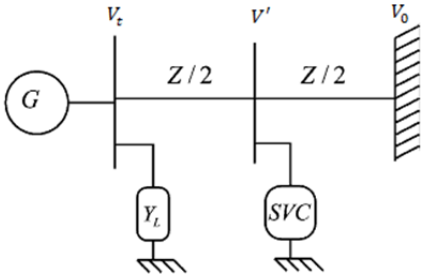

Fig. 1 Single machine infinite bus system with SVC

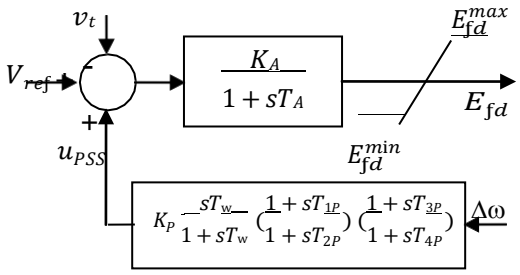

Fig. 2 IEEE Type-ST1 excitation system with lead-lag PSS

C. SVC-Based Stabilizer

The block diagram of an SVC with a lead-lag compensator is shown in Fig.3. The susceptance B_{SVC} of the SVC can be expressed as:

$$\dot{B}_{SVC} = (K_C(B_{ref} - u_{SVC}) - B_{SVC})/T_C \tag{10}$$

Where K_C and T_C are the gain and time constant of the SVC; B_{ref} is the reference susceptance of SVC. A conventional lead-lag controller as shown in Fig.3 is installed in the feedback loop to generate the SVC stabilizing signal u_{SVC} .

D. Linearized Model

The linearized power system model can be obtained by linearizing the expressions of i_d and i_q and substituting into the linear form of Eqs. (1) −(10). It can be represented in the state-space form $\dot{X} = AX + HU$, as follows:

$$\begin{bmatrix} \Delta\dot{\delta} \\ \Delta\dot{\omega} \\ \Delta\dot{E}'_q \\ \Delta\dot{E}_{fd} \end{bmatrix} = \begin{bmatrix} 0 & 377 & 0 & 0 \\ -\frac{K_1}{M} & -\frac{D}{M} & -\frac{K_2}{M} & 0 \\ -\frac{K_4}{T'_{d0}} & 0 & -\frac{K_3}{T'_{d0}} & \frac{1}{T'_{d0}} \\ -\frac{K_A K_5}{T_A} & 0 & -\frac{K_A K_6}{T_A} & -\frac{1}{T_A} \end{bmatrix} \times \begin{bmatrix} \Delta\delta \\ \Delta\omega \\ \Delta E'_q \\ \Delta E_{fd} \end{bmatrix} + \begin{bmatrix} 0 & 0 \\ 0 & -\frac{K_{pB}}{M} \\ 0 & -\frac{K_{qB}}{T'_{d0}} \\ \frac{K_A}{T_A} & -\frac{K_A K_{vB}}{T_A} \end{bmatrix} \begin{bmatrix} \Delta u_{PSS} \\ \Delta B_{SVC} \end{bmatrix} \tag{11}$$

Where the state vector X is $[\Delta\delta, \Delta\omega, \Delta E'_q, \Delta E_{fd}]^T$ and the control vector U is $[\Delta u_{PSS}, \Delta B_{SVC}]^T$. The linearization constants $K_1 - K_6, K_{pB}, K_{qB}$ and K_{vB} are defined as

$$\begin{aligned} K_1 &= \partial P_e/\partial\delta, K_2 = \partial P_e/\partial E'_q, K_{pB} = \partial P_e/\partial B_{SVC} \\ K_4 &= \partial E_q/\partial\delta, K_3 = \partial E_q/\partial E'_q, K_{qB} = \partial E_q/\partial B_{SVC} \\ K_5 &= \partial v_t/\partial\delta, K_6 = \partial v_t/\partial E'_q, K_{vB} = \partial v_t/\partial B_{SVC} \end{aligned} \tag{12}$$

ISSN: 2356-5608

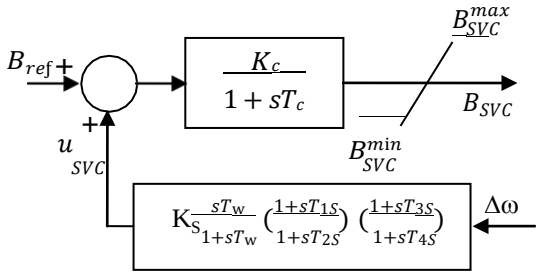

Fig. 3 Block diagram of SVC with lead-lag controller

III. THE PROPOSED APPROACH

A. Stabilizer Design

The lead-lag structure of PSS and SVC controllers is considered in this study. It's the commonly used structure. The washout time constant T_W and the two time constants of PSS and SVC: T_{2P} ,T_{4P} ,T_{2S} and T_{4S} are usually prespecified [12]. The controllers gain K_P and K_S and the time constants T_{1P} ,T_{3P} ,T_{1S} and T_{3S} are to be optimized. Typical ranges of the optimized parameters are [0.01−100] for K and [0.01−1] for the time constants.

In the stabilizer design process, the performance index is the integral of time multiplied absolute value of the error (ITAE) expressed as follows:

$$ITAE = \min(F_1, F_2) \tag{13}$$

Where

$$F_1 = \int_0^{t_1} |\Delta\omega(t, X)| t dt \tag{14}$$

$$F_2 = \int_0^{t_1} |\Delta v_t(t, X)| t dt \tag{15}$$

In the above equations:

- $|\Delta\omega(t, X)|$ and $|\Delta v_t(t, X)|$ are the absolute values of the speed deviation and terminal voltage deviation .
- t_1: time simulation domain.
- X : vector of decision variables represented by the parameters of the controllers to be optimized.

The constraints of the design problem are the parameters bounds.

$$\begin{aligned} K_P^{\min} \le K_P \le K_P^{\max} \\ T_{1P}^{\min} \le T_{1P} \le T_{1P}^{\max} \\ T_{3P}^{\min} \le T_{3P} \le T_{3P}^{\max} \\ K_S^{\min} \le K_S \le K_S^{\max} \\ T_{1S}^{\min} \le T_{1S} \le T_{1S}^{\max} \\ T_{3S}^{\min} \le T_{3S} \le T_{3S}^{\max} \end{aligned} \tag{16}$$

B. Controllability Measure

In this paper, for measuring the controllability of the electromechanical modes by a given input, the SVD is employed. Participation factor technique [13] is applied to identify the mode of oscillations related to machine inertia, called electromechanical modes.

Mathematically, if G is an $m \times n$ complex matrix, then there exist unitary matrices W and V with dimensions of $m \times m$ and $n \times n$, respectively, such that G can be written as

$$G = W \Sigma V^H \tag{17}$$

Where

$$\Sigma = \begin{bmatrix} \Sigma_1 & 0 \\ 0 & 0 \end{bmatrix} \tag{18}$$

$$\Sigma_1 = \text{diag}(\sigma_1,...,\sigma_r) \text{ with } \sigma_1 \ge ... \ge \sigma_r \ge 0$$

Where $r = \min\{m, n\}$ and $\sigma_1,...,\sigma_r$ are the singular values of G .

The minimum singular value σ_r represents the distance of the matrix G from all the matrices with a rank of r −1 . This property can be utilized to quantify modal controllability [14]. In this study, the matrix H in Eq. (11) can be written as $H = [h_1, h_2]$, where h_i is the column of matrix H corresponding to the ith input. The minimum singular value $\sigma_{\min}$ of the matrix $[\lambda I - A \quad h_i]$ indicates the capability of the ith input to control the mode associated with the eigenvalue λ . As a matter of fact, higher the $\sigma_{\min}$, the higher the controllability of this mode by the input considered. Having been identified, the controllability of the electromechanical mode can be examined with both inputs in order to identify the most effective one to control that mode.

IV. MOPSO APPROACH

This approach is population-based, it uses an external memory, called repository, and a geographically-based approach to maintain diversity. MOPSO is based on the idea of having a global repository in which every particle will deposit its flight experiences after each flight cycle. The general algorithm of MOPSO can be described in steps as follows [15]:

Step 1: Initialize an array of particles with random positions POP and their associated velocities VEL .
Step 2: Evaluate the fitness function of each particle.
Step 3: Store the positions of the particles that represent nondominated vectors in the repository REP .
Step 4: Generate hypercubes of the search space explored so far, and locate the particles using these hypercubes as a coordinate system.
Step 5: Initialize the memory of each particle.
Step 6: Compute the speed of each particle using the following expression:

$$\begin{aligned} VEL(i) = \chi[VEL(i) + \phi_1 r_1 (PBEST(i) - POP(i)) \\ + \phi_2 r_2 (REP(h) - POP(i))] \end{aligned} \tag{19}$$

Here ϕ_1 and ϕ_2 are weights affecting the cognitive and social factors, respectively; r_1 and r_2 are random numbers in the range [0-1].

χ is the constriction factor that ensures convergence which is calculated as in Eq. (20):

ISSN: 2356-5608

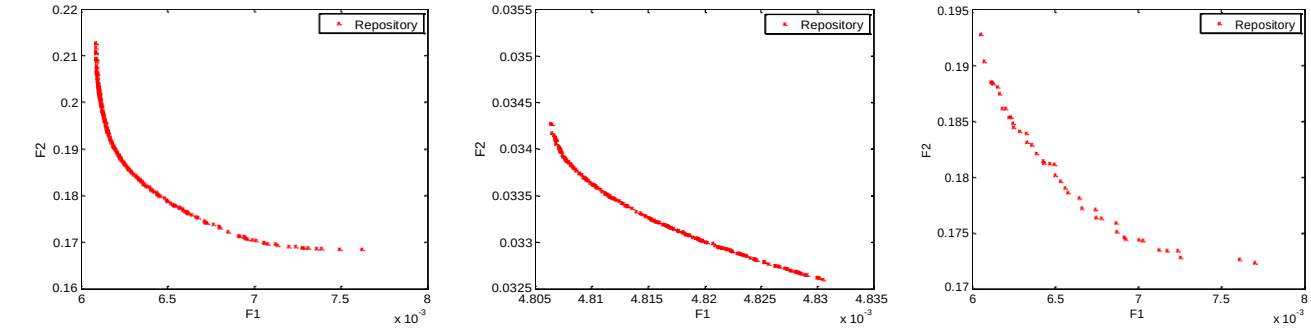

(a) (b) (c)

Fig. 4 Pareto fronts produced by MOPSO. (a) PSS only, (b) SVC only, (c) PSS and SVC

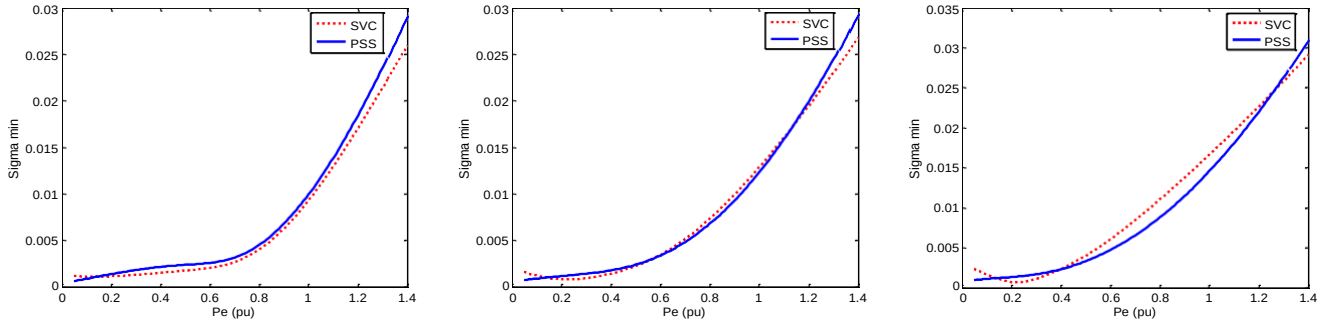

(a) (b) (c)

Fig. 5 Minimum singular value with loading variations. (a) $Q=-0.4$ pu , (b) $Q=0.0$ pu , (c) $Q=0.4$ pu

$$\chi = \begin{cases} \dfrac{2k}{\left|2-\varphi-\sqrt{\varphi^2-4\varphi}\right|} & \text{if } \varphi \geq 4 \\ k & \text{if } 0 \leq \varphi \leq 4 \end{cases} \quad (20)$$

Where $0 \leq k \leq 1$ and $\varphi = \phi_1 + \phi_2$ (21)

PBEST (i) is the best position that the particle i has had; *REP*(h) is a value that is taken from the repository; the index h is selected by applying roulette-wheel selection.

Step 7: Update the position for each particle

$$POP(i) = POP(i) + VEL(i) \quad (22)$$

Step 8: Maintain the particles within the search.

Step 9: Evaluate each of the particles in *POP* .

Step 10: Update the contents of *REP* together with the geographical representation of the particles within the hypercubes.

Step 11: Update the particle's position using Pareto dominance.

Step 12: Repeat Step 6-11 until a stopping criterion is satisfied or the maximum number of iterations is reached.

V. RESULTS AND DISCUSSIONS

A. Loading Conditions and Proposed Stabilizers

In this study, the proposed approach has been implemented on a SMIB system. The system data is given in appendix. To assess the robustness and effectiveness of the proposed stabilizers, three different loading conditions, given in Table I, were considered.

TABLE II

LOADING CONDITIONS

Loading	$P(pu)$	$Q(pu)$
Nominal	1.0	0.015
Light	0.3	0.015
Heavy	1.1	0.4

The Pareto fronts produced by the MOPSO when PSS and SVC controller designed individually and through coordinated design are shown in Fig.4. The final settings of the optimized parameters for the proposed stabilizers are given in Table II.

TABLE II

OPTIMAL PARAMETER SETTINGS OF THE PROPOSED STABILIZERS

	Individual design		**Coordinated design**	
	PSS	**SVC**	**PSS**	**SVC**
K	22.797	99.213	45.713	98.733
T_1	0.3180	0.7529	0.1552	0.5969
T_2	0.1000	0.3000	0.1000	0.3000
T_3	–	0.0110	–	0.3692
T_4	–	0.3000	–	0.3000

B. Electromechanical Mode controllability Measure

The controllability of the electromechanical mode from each input signal is measured through estimation of the minimum singular value σ_{min} . Fig.5 shows σ_{min} with the

ISSN: 2356-5608

TABLE III

SYSTEM EIGENVALUES WITH THE PROPOSED STABILIZERS

Controllers	**Nominal loading**	**Light loading**	**Heavy loading**
Without Controller	0.2951 ± j4.9596*	-0.0090 ± j4.8527*	0.4848 ± j3.6950*
	-0.0594**	0.0019**	-0.1301**
	-10.3930 ± j3.2837	-10.0888 ± j3.8317	-10.5826 ± j3.6932
PSS only	- 2.3148 ± j3.5266*	- 1.2171 ± j4.9201*	- 1.4002 ± j2.9133*
	0.5487**	0.2401**	0.4332**
	-2.9297 ± j8.5356	-5.5891 ± j5.6941	-3.8745 ± j8.1463
	- 19.7013	- 16.5809	- 19.6372
	- 0.2054	- 0.2023	- 0.2090
SVC only	- 1.0830 ± j5.1941*	- 0.1546 ± j4.7631*	- 1.4436 ± j3.9090*
	0.2041**	0.0324**	0.3464**
	- 3.9930 ± j3.8253	- 9.0674 ± j2.1672	- 3.1974 ± j3.0554
	- 20.3324	- 19.9374	- 20.7169
	- 13.6683	- 5.8162	- 12.5664
	- 2.7085	- 2.6651	- 4.2928
	- 0.2012	- 0.1998	- 0.2043
PSS & SVC	- 2.8524 ± j2.9676*	- 1.4290 ± j5.2880*	- 2.1963 ± j1.4533*
	0.6930**	0.2609**	0.8340**
	- 5.7110 ± j10.7275	- 6.6258 ± j5.1334	- 6.3730 ± j10.9833
	- 2.9018± j0.2972	- 3.1128 ± j0.3391	- 16.4956 ± j2.8828
	- 17.8181	- 20.3940	- 3.9487
	- 16.1004	- 14.1287	- 2.7568
	- 0.2134	- 0.2047	- 0.2271
	- 0.2000	- 0.2000	- 0.2000

* Electromechanical mode ** Damping ratio

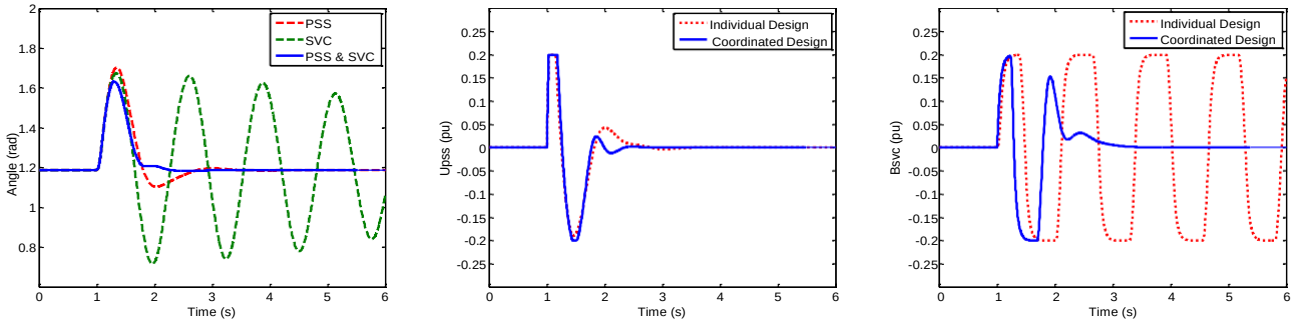

(a) (b) (c)

Fig. 6 System response for 6-cycle fault disturbance with nominal loading. (a) Rotor angle response; (b) PSS stabilizing signal; (c) B_{SVC} variation

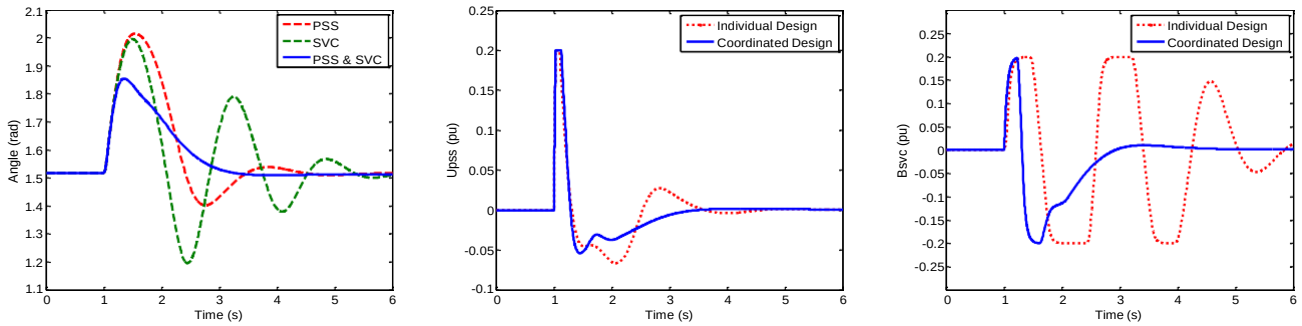

(a) (b) (c)

Fig. 7 System response for 3-cycle fault disturbance with heavy loading. (a) Rotor angle response; (b) PSS stabilizing signal; (c) B_{SVC} variation

ISSN: 2356-5608

variation of system loading conditions over the range of $P_e = [0.05 - 1.4]$ pu and $Q = \{-0.4, 0.0, 0.4\}$ pu. It can be seen that the electromechanical mode controllability is almost the same in case of PSS and SVC. In addition, the mode controllability changes almost linearly with the system loading.

C. Eigenvalue Analysis and Nonlinear Simulation Results

The proposed stabilizers were tested under different disturbances and loading conditions for verification and completeness.

(a) Nominal loading $(P, Q) = (1.0, 0.015)$pu with 6-cycle three-phase fault.
(b) Light loading $(P, Q) = (0.3, 0.015)$pu with 6-cycle three-phase fault.
(c) Heavy loading $(P, Q) = (1.1, 0.4)$pu with 3-cycle three-phase fault.

The system eigenvalues without and with the proposed stabilizers at these loading conditions are given in Table III. It is clear that the system stability is greatly improved with the proposed stabilizers. In addition, we can perceive that the coordinated design outperforms the individual design at all points considered since the damping ratios of the electromechanical modes at all points are greatly improved.

On the other hand, we have carried out the nonlinear time domain simulations at the disturbances and the loading conditions specified above. The system responses with 6-cycle then with 3-cycle fault disturbances at the nominal loading and at a heavy loading conditions, respectively are shown in Fig.6 and Fig.7. It is clear that the coordinated design approach provides the best damping characteristics and enhances greatly the first swing stability. In addition, it can be seen that the control effort is greatly reduced with the coordinated design approach. This confirms the potential of the proposed approach to enhance the system dynamic stability.

VI. CONCLUSION

In this study, the power system stability enhancement via PSS and SVC-based stabilizer when applied independently and also through coordinated design was discussed and investigated. The design problem is converted to an optimization problem which is solved by MOPSO. In order to obtain the best system response, objective function namely ITAE is considered. In addition, SVD was employed to evaluate the electromechanical mode controllability and to assess the effectiveness of the proposed stabilizers. The eigenvalue analysis and nonlinear simulation results show the effectiveness and robustness of the proposed stabilizers to enhance the system stability for a wide range of operating conditions.

APPENDIX

The test system parameters are: All data are in pu unless specified otherwise.

Machine: $D = 0$; $x_d = 0.973$; $x_q = 0.55$; $x'_d = 0.19$; $M = 9.26$

$T'_{d0} = 7.76$ s; $f = 60$ Hz; $v_t = 1.05$

Excitation System: $K_A = 50$; $T_A = 0.05$ s

Transmission line: $R = -0.034$; $X = 0.997$

$G = 0.249$; $B = 0.262$

REFERENCES

[1] P.Kundur, Power System Stability and Control, McGraw-Hill, 1994.
[2] N.G. Hingorani, FACTS-Flexible AC Transmission System, in: Proceedings of the Fifth International Conference on AC and DC Power Transmission, vol. 345, IEE Conference Publication, 1991, pp. 1–7.
[3] M. A. Abido, "Pole placement technique for PSS and TCSC-based stabilizer design using simulated annealing," Electrical Power and Energy Systems, Vol. 22, pp. 543-555, 2000.
[4] Y. L. Abdel-Magid and M. A. Abido, "Robust Coordinated Design of Excitation and TCSC-based Stabilizers using Genetic Algorithms," International Journal of Electrical Power & Energy Systems, Vol. 69, No. 2-3, pp. 129-141, 2004.
[5] S. Panda, N. P. Padhy and R. N. Patel, "Robust Coordinated Design of PSS and TCSC using PSO Technique for Power System Stability Enhancement," J. Electrical Systems Vol. 3, No. 2, pp. 109-123, 2007.
[6] Mahran AR, Hogg BW and El-Sayed ML, "Coordinated control of synchronous generator excitation and static VAR compensator," IEEE Trans Energy Conv 1992; 7:615-22.
[7] Rahim A and Nassimi S, "Synchronous generator damping enhancement through coordinated control of exciter and SVC," IEE Proc Gener Transm Distrib 1996; 143(2):211-8.
[8] Y.L.Abdel-Magid and M.A.Abido, "Robust coordinated design of excitation and TCSC-based stabilizers using genetic algorithms," International Journal of Electrical Power & Energy Systems, vol.69, no.2-3, pp.129-141.2004.
[9] James Kennedy and Russel C.Eberhart. Swarm Intelligence. Morgan Kaufmann Publishers, San Francisco, California, 2001.
[10] Bland JA, Dawson G. Tabu search and design optimization. Comput-Aided Des 1991; 23(3):195-201.
[11] Carlos A. Coello Coello and al, "Handling Multiple Objectives with Particle Swarm Optimization," IEEE Transactions on Evolutionary Computation, Vol. 8, No.3, pp.256-279, June 2004.
[12] M. A. Abido, "A novel approach to conventional power system stabilizer design tabu search," Int. J. Electrical Power and Energy Syst., 21(6), pp. 443-454, 1999.
[13] Y.Y. Hsu and C.L. Chen, Identification of optimum location for stabilizer applications using participation factors, IEE Proc, Part C 1987; 134(3):238-44.
[14] Hamdan AMA, An investigation of the significance of singular value decomposition in power system dynamics. Int J Electr Power Energy Syst 1999; 21:417-24.
[15] Carlos A. Coello Coello and Maximino Salazar Lechuga, "MOPSO: A Proposal for Multiple Objective Particle Swarm Optimization," IEEE Transactions on Evolutionary Computation, Vol. 2, No.3, pp.1051-1056, May 2002.

ISSN: 2356-5608